Karlsruhe Institute of Technology

Elektrotechnisches Institut (ETI)
Prof. Dr.-Ing. Michael Braun
Prof. Dr.-Ing. Martin Doppelbauer
Prof. Dr.-Ing. Marc Hiller
Kaiserstr.12. 76131 Karlsruhe

Elektrotechnisches Institut

Title:	Expanding the operating range of permanent magnet synchronous motors by using the optimum number of phases
Authors:	Miriam Boxriker, Johannes Kolb, Martin Doppelbauer
Institute:	Karlsruhe Institute of Technology (KIT) Elektrotechnisches Institut (ETI) Hybrid Electric Vehicles (HEV)
Type:	Conference Proceedings
Published at:	18th European Conference on Power Electronics and Applications, EPE 2016 ECCE Europe, Karlsruhe, Germany Publisher: IEEE, Piscataway (NJ) Year: 2016 ISBN: 978-90-75815-24-5 Pages: 1-8
Hyperlinks:	DOI: https://doi.org/10.1109/EPE.2016.7695597

Expanding the Operating Range of Permanent Magnet Synchronous Motors by Using the Optimum Number of Phases

Miriam Boxriker, Johannes Kolb[‡], Martin Doppelbauer
Karlsruhe Institute of Technology (KIT)
Elektrotechnisches Institut (ETI) - Hybrid Electric Vehicles (HEV)
Kaiserstr. 12, 76131 Karlsruhe, Germany
Phone: +49 (0) 721 608-42700
Fax: +49 (0) 721 608-42921
Email: miriam.boxriker@kit.edu
URL: www.eti.kit.edu
[‡] Schaeffler Technologies AG & Co. KG - SHARE at KIT

Keywords

≪Electrical machine≫, ≪Multiphase drive≫, ≪Permanent magnet motor≫, ≪Electric Vehicle≫, ≪Efficiency≫, ≪Pulse Width Modulation (PWM)≫.

Abstract

A holistic approach to determine the optimum number of phases m of an m-phase motor in combination with an m-leg inverter for electric vehicle applications is presented. The optimum offers a significant improvement of the torque and power by approximately 9.6% over the whole operating range in comparison to a 3-phase motor and therefore enhances the power and torque density without expanding the design parameters of the machine.

Introduction

Usually, 3-phase permanent magnet synchronous motors (PSM) with buried magnets are used in drivetrains for electric vehicles (EV). These PSMs offer a high power density and high efficiency as well as an adequate operating range for EVs including a large field weakening range. As the operating distance is crucial to the EVs, the weight and the costs of batteries and drivetrain components have to be reduced. Multi-phase electric machines are an interesting alternative to conventional three-phase machines to meet these targets [1]. The torque of a machine at the same volume is enhanced by using a larger number of phases [2]. Simultaneously, the torque ripple can be minimized [3].

According to these aspects of the electric machine, multi-phase inverters have been discussed and their advantages regarding control and output voltage have been compared to three-phase inverters [4]. A better utilization of the DC link voltage U_{DC} is possible and harmonics in the phase current could be reduced. In this paper, both components of a drivetrain for an EV are taken into account in order to evaluate the increase of the torque-speed range enabled by multiple phases of motor and power electronics. The following analysis identifies the optimum number of phases to utilize the limited space. The considerations are restricted to an odd phase number, because the phase shift is then uniformily distributed by $2\pi/m$ [5].

First, the benefits and challenges for the power electronics realized by an m-leg inverter regarding its losses and chip area are discussed. An m-phase space vector pulse width modulation for driving the semiconductor switches is examined with respect to the possible utilization of U_{DC} and the common mode voltage u_0 in the next Section. After that, the limit values of the motor characteristics are benchmarked by the winding factor and the harmonic content of the phase currents. Due to the results of each

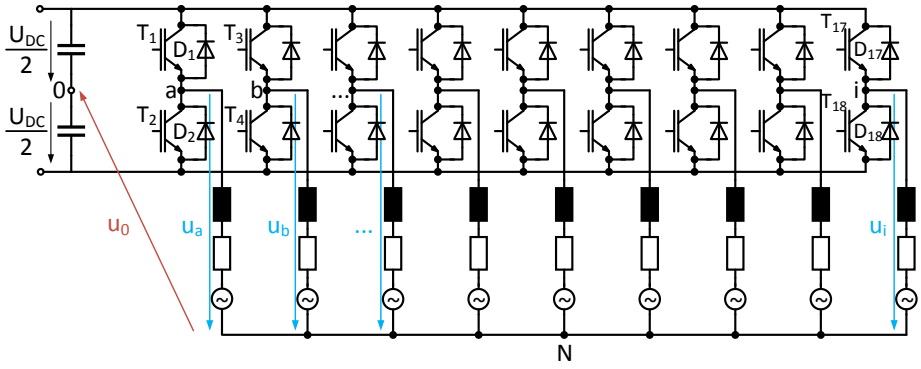

Fig. 1: 9-leg inverter with a common floating neutral point N

Section, it is shown that it is not promising to increase the phase number above a certain value. Finally, the choice of the optimum number of phases in combination with the electromagnetic finite element simulation of the motor shows a significant increase in the maximum torque over the complete speed range. This expansion of the operating range yields higher power density of the entire drive system.

Power Electronics

For operating the m-phase motor, an extension of the three-leg inverter to an m-leg inverter is necessary, where all phases of the motor are star-connected at the neutral point N. Consequently, the inverter itself consists of m half bridges with transistors e.g. IGBTs (insulated-gate bipolar transistors) $\mathrm{T}_1 - \mathrm{T}_{18}$ and free-wheeling diodes $\mathrm{D}_1 - \mathrm{D}_{18}$, as depicted in Fig. 1.

With a simple power loss model of the used semiconductors, the quantity of the losses depending on the phase number m is determined. It is assumed that the total chip area of the semiconductors is kept constant for every different number of m, which means that the chip area for one pair of IGBT and diode is reduced by the factor m, while the current density is constant, since the current per phase $I(m)$ is proportional by $1/m$ and therefore the total current is $I_\Sigma = m \cdot I(m)$. Hence, the active power P_{el} becomes independent of m, as U_{DC} is constant:

$$P_{\mathrm{el}} = m \cdot U \cdot I\,(m) \cos\,(\varphi) = U \cdot I_\Sigma \cdot \cos\,(\varphi) \tag{1}$$

with the power factor $\cos\,(\varphi)$ and the phase voltage U. On a physical consideration on the power electronics level by using IGBTs and diodes with a smaller chip area, the resistances of IGBT and diode increase proportional by m, as the resistance per area $r_{\mathrm{T/D}}$ is constant, and the recovery charge of a diode decreases with $1/m$, while the threshold voltage $U_{\mathrm{T/D0}}$ remains approximately constant [6]. As the switching energies can be calculated in a worst-case assumption by the area spanned by the linearization of rise and fall of voltage and current [6, 7] while the switching time stays constant, the switching energy reduces with $1/m$. If the current changing speed stays the same while reducing the current, the decrease is even greater than $1/m$.The losses P_{v} in an m-leg inverter with IGBT-semiconductors consist primarily and in a good approximation of conduction and switching losses [7]:

$$P_{\mathrm{v}} = m \cdot \left(\underbrace{U_{\mathrm{T0}} \cdot k_1 \cdot \frac{I_\Sigma}{m} + \left(r_{\mathrm{T/D}} \cdot m\right) \cdot k_2 \cdot \left(\frac{I_\Sigma}{m}\right)^2}_{\text{conduction losses per leg} \propto 1/m} + \underbrace{\frac{f}{\pi} \cdot k_3 \cdot \frac{I_\Sigma}{m}}_{\text{switching losses per leg} \propto 1/m} \right) \tag{2}$$

with the switching frequency f and the operating point dependent values k_1, k_2, k_3, which are constant in this case. Since the conduction losses and switching losses per leg are decreasing by $1/m$, they become

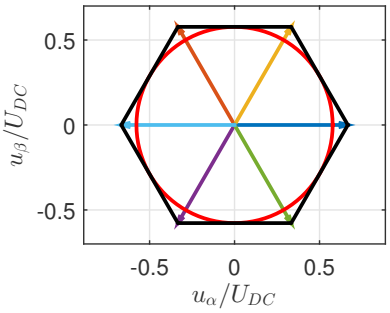

Fig. 2: Inner circle of the polygon with $2m$ edges for $m = 3$ characterizes the limitation of the voltage space vector $\underline{u}_\mathrm{n}$ for the fundamental frequency

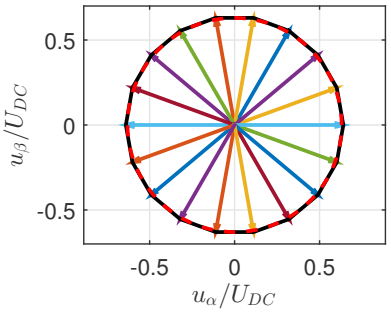

Fig. 3: Inner circle of the polygon with $2m$ edges for $m = 9$ is bigger than for $m = 3$

constant for m phases. Consequently, the increase in phases does not effect the losses of the power electronics in case of these approximations and therefore, they do not need taken into account for the further considerations.

M-Phase Space Vector Pulse Width Modulation (SVPWM)

In order to achieve a high utilization of U_DC, a space vector pulse width modulation (SVPWM) is examined [4]. Here, the amplitude of the phase voltage $\hat{u}$ regarding the fundamental frequency is limited to the inner circle of the polygon. This polygon is spanned by the $2m$ edges of the maximum space vectors according to the examples with $m = 3$ in Fig. 2 and $m = 9$ in Fig. 3. As it can be seen in the figures, the more phases there are the more edges of the polygon exist which offer a better approximation of the inner circle resulting in a larger radius. This advantage of an improved utilization of the DC link voltage U_DC due to an m-leg inverter and an m-phase machine is shown in [3, 4]. In this paper, the reachable limit for this inverter with SVPWM is examined further. There are 2^m space vectors which can be calculated by the Clarke-transformation [8] of the voltage of each leg with the values of $\pm U_\mathrm{DC}/2$ shifted by the phase angle of $2\pi/m$. Since the maximal attainable modulation factor of a SVPWM is requested, the space vectors $\underline{u}$ with the maximum magnitude are deduced and evaluated. The space vectors $\underline{u}$ can be described as

$$\underline{u} = \frac{2}{m} \sum_{k=1}^{m} \alpha_k e^{j\frac{2\pi}{m}(k-1)} \tag{3}$$

with $\alpha_k = \pm U_\mathrm{DC}/2$. By examining (3), it is obvious that the maximum space vectors can be calculated if $(m-1)/2$ vectors with an angle β with $\pi/2 \leq \beta \leq 3/2\pi$ to the resulting space vector $\underline{u}$ have a negative prefactor α_k while the prefactors α_k of the other $(m+1)/2$ vectors are positive. By normalizing (3) by U_DC and rearranging it to represent only the space vector with maximal length, (3) becomes

$$\underline{u}' = \sum_{k=1}^{m} \frac{1}{m} e^{j\frac{\pi}{m}(k-\frac{m+1}{2})} \tag{4}$$

The maximum magnitude of $\underline{u}$ for an infinite number of phases m therefore yields

$$\lim_{m\to\infty} \left|\underline{u}'\right| = \lim_{m\to\infty} \sqrt{\left(\sum_{k=1}^{m} \frac{\cos\left(\frac{\pi}{m}\left(k-\frac{1}{2}\right)\right)}{m}\right)^2 + \left(\sum_{k=1}^{m} \frac{\sin\left(\frac{\pi}{m}\left(k-\frac{1}{2}\right)\right)}{m}\right)^2} = \frac{2}{\pi} \tag{5}$$

By the SVPWM, the inner circle of the polygon with $2m$-edges spanned by the space vectors can be realized as output phase voltage regarding the fundamental frequency. The formula of the inner circle $r_{\max}$ for $m \to \infty$ is:

$$r_{\max,\mathrm{m}\to\infty} = \lim_{m\to\infty} \left(|\underline{u}'| \cos\left(\frac{\pi}{2m}\right)\right) = \frac{2}{\pi} \cdot 1 = \frac{2}{\pi} \tag{6}$$

That means that $2/\pi \cdot U_{\mathrm{DC}}$ is the theoretical limit of the amplitude of the phase voltage. This is the same fundamental phase voltage, which can be achieved by $2m$-step mode respectively block commutation but with higher harmonics [4]. In Table I the maximum possible modulation index r_{max} by space vector modulation is listed for different numbers of m. While the magnitude of the space vector $\underline{u}$ is decreasing if the number of phases m rises, the possible modulation index r_{max} is increasing until the limit of $2/\pi$ is reached.

Besides, a zero-component, the common mode voltage u_0, belongs to each space vector. u_0 can be calculated with

$$u_0 = \frac{1}{m} \sum_{k=1}^{m} \alpha_k \tag{7}$$

Since m is an odd number and u_0 of the maximum vector $\underline{u}$ consists of $(m-1)/2$ positive and $(m-1)/2$ negative α_k, (7) becomes

$$u_0(\underline{u}) = \pm \frac{1}{m} \frac{U_{\mathrm{DC}}}{2} \tag{8}$$

That means, that the peak-to-peak-value of u_0, $u_{0,pp}$, is dependent on $1/m$. Compared to a 3-leg-inverter, $u_{0,pp}$ of a 9-leg-inverter with the described SVPWM can be reduced by 67%. This leads to smaller capacitive leakage currents, which cause current stress in bearings resulting, for example, in degradation [9]. In Table II the relation of m and $u_{0,pp}$ and the percentage gain representing the reduction of the peak-to-peak-value is listed.

Table I: The possible modulation by SVPWM regarding $|\underline{u}|_{\max}$ and inner circle radius $r_{\max}$.

m phases	$\lvert\underline{u}\rvert_{\max}$	$r_{\max}$	Percentage
3	0.667	0.577	90.7%
5	0.647	0.616	96.7%
7	0.642	0.626	98.3%
9	0.640	0.630	99.0%
11	0.639	0.632	99.3%
∞	$2/\pi \approx 0.6366$	$2/\pi$	100%

Table II: The peak-to-peak-value $u_{0,pp}$ of $\underline{u}$ and the percentage gain compared to $m = 3$.

m phases	$u_{0,pp}$	Percentage
3	$0.333U_{\mathrm{DC}}$	0%
5	$0.200U_{\mathrm{DC}}$	40.0%
7	$0.143U_{\mathrm{DC}}$	57.1%
9	$0.111U_{\mathrm{DC}}$	66.7%
11	$0.091U_{\mathrm{DC}}$	72.7%
∞	0	100%

Motor Characteristics: Number of Slots, Winding Factor and Harmonics

In the previous Sections, it has been shown that there are limits for the losses of the power electronics as well as for the maximum possible modulation index. In order to find the optimum configuration of the motor, the interaction of the number of slots N, the winding factor ξ and the occurring harmonics

are examined further. If the design is built of distributed full-pitch windings, the winding factor of the fundamental wave ${}^1\xi$ [5] is calculated by

$${}^1\xi = \frac{\sin\left(\frac{\pi q p}{N}\right)}{q \sin\left(\frac{\pi p}{N}\right)} \tag{9}$$

with the number of pole pairs p and the number of slots per pole and phase q. When q and m tend to infinity in order to calculate the lowest winding factor possible, equation (9) becomes:

$$\lim_{m\to\infty}\left(\lim_{q\to\infty} {}^1\xi\right) = \lim_{m\to\infty}\left(\frac{2m \sin\left(\frac{\pi}{2m}\right)}{\pi}\right) = 1 \tag{10}$$

Additionally, it becomes evident that not only the behavior of ${}^1\xi$ is significantly improved by increasing m but also occurring harmonics of air-gap field can be reduced. The effects of these harmonics can be taken into account with the double-linkage leakage σ_o [10]:

$$\sigma_o = \sum_{\nu\neq 1} \frac{1}{\nu}\left(\frac{{}^\nu\xi}{{}^1\xi}\right)^2 \tag{11}$$

Equation (11) was solved in [10] for $m \to \infty$ and different values for q. It was stated that (11) converges towards zero for $m \to \infty$. Furthermore, it was shown that σ_o is decreasing with q but even more with m and that it is therefore advantageous to increase m at the expense of q. In Table III, this relation is depicted, whereas $\sigma_{o,max}$ is the maximum σ_o for a certain m with $q = 1$. It is evident that with a higher phase number m, the damping of the fundamental wave is reduced and simultaneously the occurring higher harmonics can be lowered significantly. Yet, each of them is limited.

Table III: The relation of m, the maximum double-linkage leakage $\sigma_{o,max}$, ${}^1\xi(q\to\infty)$ and N.

m phases	$\sigma_{o,max}$	${}^1\xi(q\to\infty)$	N for $p=2$
3	0.0966	0.955	12
5	0.0336	0.984	20
7	0.0170	0.992	28
9	0.0102	0.995	36
11	0.0068	0.997	44
∞	0	1	∞

Determining the optimal phase number

The limits presented before are used to identify the optimum number of phases by introducing a quality criterion J is defined to judge all influences for this purpose. In order to seperate positive $\delta_P(m)$ and negative influences $\delta_N(m)$, J is divided into two parts:

$$J(m) = \delta_P(m) + \delta_N(m) \tag{12}$$

$\delta_P(m)$ sums up the limit values for r_{max}, $u_{0,pp}$, ${}^1\xi(q\to\infty)$ and $\sigma_{o,max}$. This is done by rearranging the equations characterizing the limits of each aspect to get the percentage change of increasing m compared to $m = 3$:

$$\delta_P(m) = q_{SVPWM}\cdot\delta_{SVPWM} + q_\xi\cdot\delta_\xi + q_{u_0}\cdot\delta_{u_0} + q_{\sigma_{o,max}}\cdot\delta_{\sigma_{o,max}} \tag{13}$$

Thus, δ_{SVPWM} characterizes this change concerning r_{max} while δ_ξ, δ_{u_0} and $\delta_{\sigma_{o,max}}$ do the same for ${}^1\xi(q\to\infty)$, $u_{0,pp}$ and $\sigma_{o,max}$ with their quality factors q_{SVPWM}, q_ξ, q_{u_0} and $q_{\sigma_{o,max}}$.

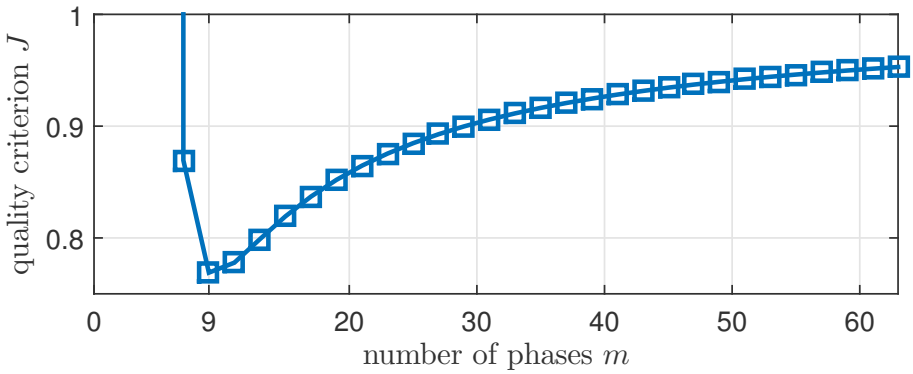

Fig. 4: The result of the quality criterion J for an odd number of phases and equally distributed quality factors, which is an exemplary choice depending on development criteria. For $m \to \infty$, J converges to 1.

As a degree of the growing costs regarding the number of slots N, the change of the slot number δ_N is introduced as

$$\delta_N(m) = 1 - \frac{N(m=3)}{N(m)} \tag{14}$$

with $m = 3,5,7,...,\infty$. The result of J for an odd number of phases and all quality factors by 0.2 is depicted in Fig. 4. J decreases for small numbers of m, since $\delta_P(m)$ is the dominating part of J, but for $m > 9$ J starts to increase until one, as the number of needed slots, δ_N, increases more strongly than the gain caused by $\delta_P(m)$.

Comparison of the simulation results of a 3-phase and 9-phase PSM

Assuming the conditions of the previous section, the optimal number of phases is $m = 9$, which is evident by considering the differences to $m = 3$. Because $\sigma_{o.max}$ is already reduced by almost 90% compared to $m = 3$, while the winding factor can only decrease to 99,5% of the maximal attainable value. Due to the 9-leg inverter with SVPWM, 99% of the maximal DC link voltage can be used compared to 90.7% with the 3-leg inverter. In contrast, the number of slots has already tripled for q and p staying the same. In order to show the expansion of the operating range by using a 9-phase machine, a 3-phase PSM with two pole pairs and 36 slots was converted into a 9-phase PSM. Only the winding of the motor has to be changed in that manner that the electric loading, the current density and the resulting number of turns w stay constant.

The simulation was performed in FLUX2D by calculating the optimal control of the current according to the "Maximum Efficiency Control" method [11]. Both designs are depicted in Fig. 5 and Fig. 6. Due

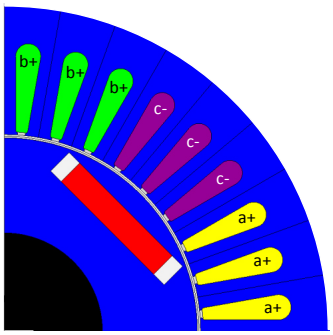

Fig. 5: Design of the 3-phase machine

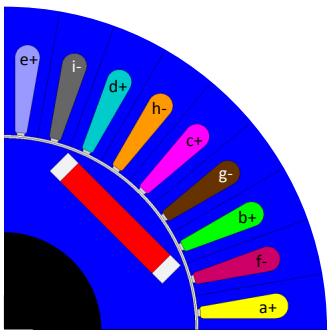

Fig. 6: Design of the 9-phase machine

to the reduced harmonics, the torque ripple is lowered and the mean torque is magnified by 5% in the normal operating range. This benefit is independent of the inverter. If the better utilization of U_{DC} by the 9-phase SVPWM is taken into account, the torque can be increased with the same DC link averagely by 12.2% in the field weakening range. The total benefit of the 9-phase motor is depicted in Fig. 7.

If the overall losses occurring in the machines of the two designs are compared and the relative reduction of the losses due to the 9-phase configuration is calculated, the result can be seen in Fig. 8. The effect can result in a loss reduction of over 15% in the field weakening area, as there is less current needed to reach the same operating point compared to the 3-phase configuration. But the benefit can be seen in a decreased manner nearly over the whole operating area.

Table IV: Electrical Machine Data

	3-phase PSM	9-phase PSM
p	2	2
q	3	1
U_{DC}	400 V	400 V
$\hat{u}$	230 V	251 V
$\hat{I}$	339 A	113 A
w	18	18

Table V: Results

	3-phase PSM	9-phase PSM
Maximal Torque	235 Nm	247 Nm
Maximal Power	101 kW	112 kW

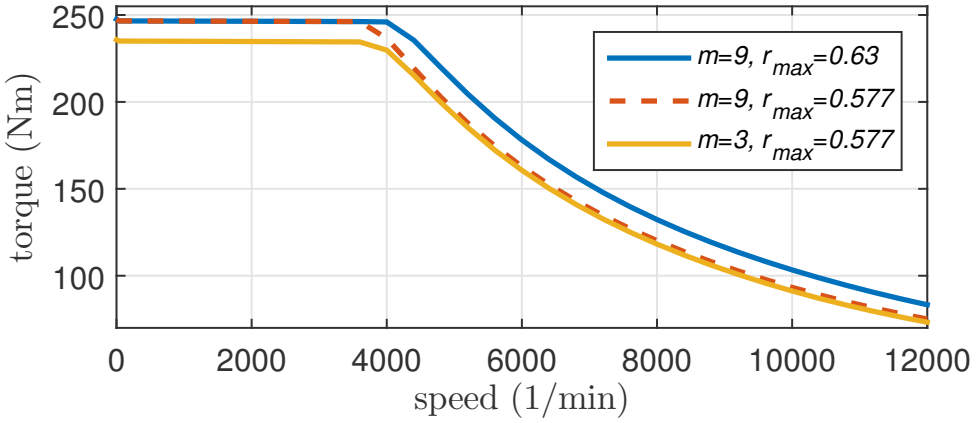

Fig. 7: The maximal torque of the 9-phase machine with the maximal SVPWM of the 9-leg inverter compared to the one of the 9-phase machine with the same phase voltage as $m = 3$ and the 3-phase machine.

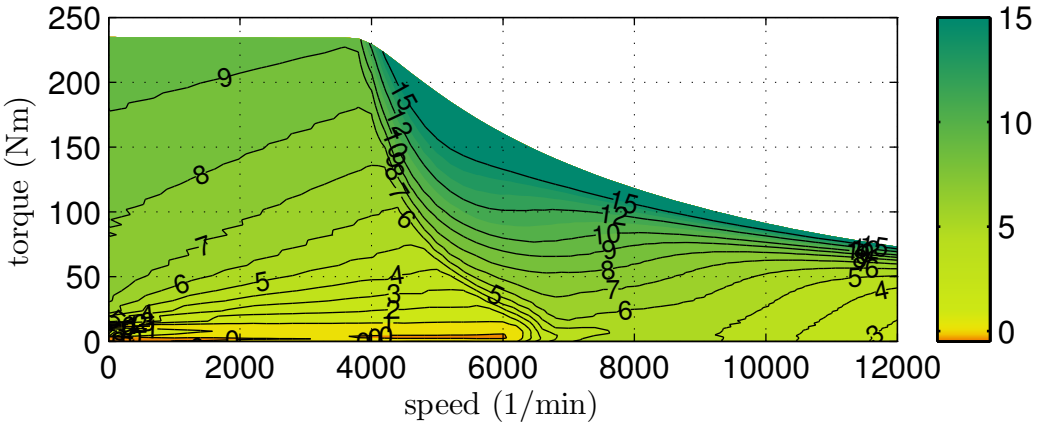

Fig. 8: The relative reduction of the losses in the machine by using a 9-phase configuration instead of a 3-phase one.

Conclusion

In this contribution, the optimum combination of an m-leg inverter with SVPWM and an m-phase PSM for EV-applications was examined. It is shown, that there are limit values for the use of the inverter as well as for the motor, which lead to an optimal interaction between the inverter and the machine. The phase number with the best cost-value-benefit with the presented quality criterion is $m = 9$. This solution is evaluated by the comparison of a 3-phase and a 9-phase machine with the same geometry. The modification of the windings to 9 phases and the use of a 9-leg inverter yield a maximum increase of the torque by 13.7% and an enhancement of the power by 10.8%. Simultaneously, the losses in the machine are reduced by maximally 27.5%

References

[1] Y. Burkhardt; A. Spagnolo; P. Lucas; M. Zavesky; P. Brockerhoff, "Design and analysis of a highly integrated 9-phase drivetrain for EV applications" in *Electrical Machines (ICEM), 2014 International Conference on*, 2014, pp. 450–456.

[2] L. Parsa, "On Advantages of Multi-Phase Machines" in *Industrial Electronics Society, 2005. IECON 2005. 31st Annual Conference of IEEE*, 2005, 6 pp.

[3] E. Levi, "Multiphase Electric Machines for Variable-Speed Applications" in *Industrial Electronics, IEEE Transactions on*, 2008, pp. 1893–1909.

[4] J.W. Kelly; E.G. Strangas; J.M. Miller, "Multiphase space vector pulse width modulation" in *Energy Conversion, IEEE Transactions on*, 2003, pp. 259–264.

[5] G. Müller; K. Vogt; B. Ponick, "Berechnung elektrischer Maschinen", *WILEY-VCH Verlag GmbH & Co. KGaA*, 6th edition, 2008.

[6] N. Mohan; T.M. Undeland; W.P. Robbins, "Power Electronics: Converters, Applications and Design" in *JOHN WILEY & SONS, INC.*, 3th edition, 2003.

[7] A. Wintrich; U. Nicolai; W. Tursky; T. Reimann, "Application Manual Power Semiconductors" by *Semikron International GmbH*, 2015.

[8] H. Späth, "Leistungsbegriffe für Ein- und Mehrphasensysteme" in *VDE-Schriftenreihe Normen verständlich Band 103*, 2nd edition, 2012.

[9] A. Muetze, "Bearing Currents in Inverter-Fed AC-Motors" dissertation in *D 17 Darmstädter Dissertationen*, 2004.

[10] H. Jordan; K. Schönbacher, "Die doppeltverkettete Streuung von mehrphasigen Mehrlochwicklungen mit Durchmesserschritt" in *Archiv f. Elektrotechnik 35(3)*, 1941, pp. 185–192.

[11] C. Mademlis; N. Margaris, "Loss minimization in vector-controlled interior permanent-magnet synchronous motor drives " in *Industrial Electronics, IEEE Transactions on*, 2002, pp. 1344–1347.